RESEARCH ARTICLE

Cyclic Rhamnosylated Elongation Factor P Establishes Antibiotic Resistance in *Pseudomonas aeruginosa*

Andrei Rajkovic,[a] Sarah Erickson,[b] Anne Witzky,[c] Owen E. Branson,[d] Jin Seo,[e] Philip R. Gafken,[f] Michael A. Frietas,[g,h] Julian P. Whitelegge,[i] Kym F. Faull,[i] William Navarre,[j] Andrew J. Darwin,[e] Michael Ibba[k]

Molecular, Cellular and Developmental Biology Program[a], Department of Chemistry[b], Department of Molecular Genetics[c], Ohio State Biochemistry Program[d], The Ohio State University, Columbus, Ohio, USA; Department of Microbiology, New York University School of Medicine, New York, New York, USA[e]; Fred Hutchinson Cancer Research Center, Proteomics Facility, Seattle, Washington, USA[f]; Comprehensive Cancer Center, The Ohio State University, Columbus, Ohio, USA[g]; Department of Molecular Virology, Immunology and Medical Genetics, The Ohio State University, Columbus, Ohio, USA[h]; Department of Psychiatry and Biobehavioral Sciences, Pasarow Mass Spectrometry Laboratory, Semel Institute for Neuroscience and Human Behavior, David Geffen School of Medicine, University of California, Los Angeles, Los Angeles, California, USA[i]; Department of Molecular Genetics, University of Toronto, Toronto, Ontario, Canada[j]; Department of Microbiology and Center for RNA Biology, The Ohio State University, Columbus, Ohio, USA[k]

ABSTRACT **Elongation factor P (EF-P) is a ubiquitous bacterial protein that is required for the synthesis of poly-proline motifs during translation. In *Escherichia coli* and *Salmonella enterica*, the posttranslational β-lysylation of Lys34 by the PoxA protein is critical for EF-P activity. PoxA is absent from many bacterial species such as *Pseudomonas aeruginosa*, prompting a search for alternative EF-P posttranslation modification pathways. Structural analyses of *P. aeruginosa* EF-P revealed the attachment of a single cyclic rhamnose moiety to an Arg residue at a position equivalent to that at which β-Lys is attached to *E. coli* EF-P. Analysis of the genomes of organisms that both lack *poxA* and encode an Arg32-containing EF-P revealed a highly conserved glycosyltransferase (EarP) encoded at a position adjacent to *efp*. EF-P proteins isolated from *P. aeruginosa* Δ*earP*, or from a Δ*rmlC*::*acc1* strain deficient in dTDP-L-rhamnose biosynthesis, were unmodified. *In vitro* assays confirmed the ability of EarP to use dTDP-L-rhamnose as a substrate for the posttranslational glycosylation of EF-P. The role of rhamnosylated EF-P in translational control was investigated in *P. aeruginosa* using a Pro_4-green fluorescent protein (Pro_4GFP) *in vivo* reporter assay, and the fluorescence was significantly reduced in Δ*efp*, Δ*earP*, and Δ*rmlC*::*acc1* strains. Δ*rmlC*::*acc1*, Δ*earP*, and Δ*efp* strains also displayed significant increases in their sensitivities to a range of antibiotics, including ertapenem, polymyxin B, cefotaxim, and piperacillin. Taken together, our findings indicate that posttranslational rhamnosylation of EF-P plays a key role in *P. aeruginosa* gene expression and survival.**

IMPORTANCE **Infections with pathogenic *Salmonella*, *E. coli*, and *Pseudomonas* isolates can all lead to infectious disease with potentially fatal sequelae. EF-P proteins contribute to the pathogenicity of the causative agents of these and other diseases by controlling the translation of proteins critical for modulating antibiotic resistance, motility, and other traits that play key roles in establishing virulence. In *Salmonella* spp. and *E. coli*, the attachment of β-Lys is required for EF-P activity, but the proteins required for this posttranslational modification pathway are absent from many organisms. Instead, bacteria such as *P. aeruginosa* activate EF-P by posttranslational modification with rhamnose, revealing a new role for protein glycosylation that may also prove useful as a target for the development of novel antibiotics.**

Received 15 May 2015 **Accepted** 19 May 2015 **Published** 9 June 2015

Citation Rajkovic A, Erickson S, Witzky A, Branson OE, Seo J, Gafken PR, Frietas MA, Whitelegge JP, Faull KF, Navarre W, Darwin AJ, Ibba M. 2015. Cyclic rhamnosylated elongation factor P establishes antibiotic resistance in *Pseudomonas aeruginosa*. mBio 6(3):e00823-15. doi:10.1128/mBio.00823-15.

Editor Susan Gottesman, National Cancer Institute

Address correspondence to Michael Ibba, ibba.1@osu.edu.

This article is a direct contribution from a Fellow of the American Academy of Microbiology.

Bacterial protein synthesis requires the activity of several essential conserved factors for initiation, elongation, termination, and recycling steps of the translation cycle. In addition to these general factors, numerous other factors control translation by interacting with the ribosome under specific conditions (1). For example, under conditions of amino acid limitation, RelA binding to ribosomes controls the stringent response, while EttA regulates protein synthesis in response to changes in the cellular ATP/ADP ratio (2–6). Other conserved translation factors have also been identified that are not essential for growth under standard laboratory conditions but are nevertheless required for efficient protein synthesis (7, 8). One notable example is the specialized translation factor elongation factor P (EF-P) that effects the translation of a particular subset of mRNAs (9, 10). In *Escherichia coli* and *Salmonella enterica*, EF-P contributes to fitness throughout vegetative growth and is required for various phenotypes, including antibiotic resistance, motility, and osmotic adaptation. EF-P activity in *E. coli* and *S. enterica* is dependent on the PoxA-catalyzed posttranslational modification of a conserved Lys residue with the amino acid (*R*)-β-Lys, the absence of which attenuates virulence.

The role of posttranslational modifications in determining the activities of translation factors is less extensively described in bacteria than in eukaryotes. Phosphorylation has been shown to negatively regulate the activities of elongation factor Tu (EF-Tu) in *Mycobacterium tuberculosis* (11) and *Bacillus subtilis* (12) and of glutamyl-tRNA synthetase in *E. coli* (13, 14), thereby limiting protein synthesis during specific phases of bacterial growth and differentiation. In *E. coli* and *S. enterica* EF-P, the (*R*)-β-Lys modification helps prevent poly-proline-induced translational stalling by increasing EF-P's binding affinity for stalled ribosomes, thereby maintaining protein homeostasis and ensuring the proper stoichiometry of different components of the proteome (7, 15–18). Eukaryotes have a conserved homolog of EF-P, known as eukaryotic initiation factor 5A (eIF5A), that also functions to alleviate poly-proline pausing but is posttranslationally modified with hypusine (19, 20). While EF-P is universally conserved in bacteria, the pathway for its posttranslational modification is not, prompting a search for alternative modification pathways.

Posttranslational glycosylation of EF-P with rhamnose from *Shewanella oneidensis* was recently reported and was shown to prevent translational stalling of a heterologously expressed *cadC* reporter gene (21). Glycosylations are primarily studied in eukaryotes, where they are thought to prevent protease degradation, promote protein folding, and provide recognition elements for cell-cell interactions (22). Bacterial glycoproteins however, are poorly understood, due to their comparatively recent emergence in the field of glycobiology (23). Modeling studies proposed that the structure of the rhamnose glycan on EF-P exists in a puckered-ring confirmation distinct from the linear geometry of (*R*)-β-Lys and hypusine (21). Despite the different chemical and structural properties of (*R*)-β-Lys and rhamnose, both are critical to EF-P's function as well as for establishing virulence, making it of considerable importance to determine how functional convergence is achieved.

In this study, with *Pseudomonas aeruginosa*, we demonstrated that the recently discovered glycosyltransferase EarP attaches a cyclic rhamnose moiety onto EF-P at the η amine position of its highly conserved R34 residue. In addition, we unambiguously established that the primary source of the sugar-nucleotide substrate is derived from the biosynthetic pathway encoded by the *rmlABCD* operon. Absence of the glycosylation leads to a significant decrease in translation of poly-proline proteins, as shown with a Pro_4-green fluorescent protein (Pro_4-GFP) *in vivo* reporter assay. A deficiency in poly-proline expression also leads to pleiotropic phenotypes and susceptibility to a host of antibiotics. Cyclic rhamnosylation of arginine represents a new mode of *N*-glycosylation in bacteria that directly contributes to antibiotic resistance for opportunistic pathogens.

RESULTS

Structure of the posttranslational modification of *P. aeruginosa* EF-P. To investigate in detail the structure of a bacterial EF-P not predicted to be modified with β-Lys, His6–EF-P was purified from *P. aeruginosa* and analyzed by mass spectrometry (MS). A high-mass spectrum was obtained for the intact His6–EF-P protein, with a Fourier transform ion cyclotron resonance (FT-ICR) mass spectrometer that measured an envelope of multiply charged ions corresponding to a monoisotopic mass of 21,913.30 Da (Fig. 1A). The calculated monoisotopic mass, based on the genomic sequence, including the hexahistadine epitope, is only 21,793.96 Da, identifying a mass difference of 146.12 Da unaccounted for in the native protein. To determine if the additional mass of 146.12 Da localized to a specific residue, His6–EF-P was digested into peptides using a Lys-C protease cocktail and analyzed on an Orbitrap Elite mass spectrometer. Lys-C digestion of His6–EF-P produced peptides with a C-terminal lysine. Fragmentation of the peptide SGRNAAVVK, by electron transfer dissociation (ETD) and higher-energy collision-induced dissociation (HCD) fragmentation, indicated that the additional mass resided on Arg32, a highly conserved residue analogous to Lys34 of *E. coli* EF-P, the site of β-Lys attachment (Fig. 1B; see also Fig. S1 in the supplemental material).

Though the FT-ICR instrument measured the mass of His6–EF-P within an error tolerance of <3 ppm, we were unable to confidently assign an elemental composition to the additional mass. However, HCD fragmentation of the modified peptide (*m*/*z* 524.29) efficiently produced fragment b-ions with and without the modification in the same ion scan. The difference between these ions was 146.058 Da (see Fig. S1 in the supplemental material). Leveraging, high mass accuracy, and resolution of the tandem MS (MS/MS) measurements enabled a determination of the elemental composition of the modification with an error tolerance of <3 ppm. From the delta mass calculation, we computed an elemental composition of $C_6H_{10}O_4$ for the unknown modification on Arg32 (calculated as 146.05791 Da; 0.6-ppm difference). The elemental composition and exact mass were then searched against databases of known posttranslational modifications and matched to a deoxyhexose—either rhamnose or fucose (24).

Though the data suggest that the modification represents a deoxyhexose, the analysis is limited to the known posttranslational modifications. To confirm whether the modification indeed represents a deoxyhexose, ETD/HCD multi-stage MS (MS^3) analysis was performed to gain structural information about the modification. ETD fragmentation of the SGRNAAVVK peptide generated a c3+ ion composed of the SerGlyArg modified tripeptide (*m*/*z* 464.246). This c3+ ion was isolated and fragmented further by HCD. From our ETD/HCD MS^3 spectra, we identified the most dominant peak as the single charged precursor ion at *m*/*z* 464.246 and identified five other abundant fragment ions measured at *m*/*z* 206.272, 301.161, 318.189, 360.199, and 446.236. On the basis of the unique series of observed mass differences consisting of 163.084 u, 146.058 u, 104.047 u, and 18.011 u, a charge-directed fragmentation pattern for the modified tripeptide was determined that was consistent with a cyclic deoxyhexose attached to the η amine of arginine (Fig. 1C). The ions with *m*/*z* values of 360.1994 and 446.2363 corresponded to neutral losses of $C_4H_8O_3$ and H_2O, respectively, and are losses characteristic of sugar moieties with a cyclic geometry (25). Ions at *m*/*z* 318.188 and 301.161 corresponded to the neutral loss of $C_6H_{12}O_4$ and $C_6H_{15}NO_4$, respectively, and are characterized by the loss of the modification either with or without the ammonia moiety, a common neutral loss observed for arginine. We determined that the ion at *m*/*z* 206.272 was a background ion by comparing the modified peptide MS^3 spectra with the MS^3 spectra of an unmodified peptide (see Fig. S2 and Table S1 in the supplemental material). The neutral losses were compared with mass spectra of the deoxyhexoses rhamnose and fucose, using the MassBank database (26). Common neutral losses were identified only with the mass spectra of rhamnose, which shared the neutral losses of H_2O and C_2H_2O, while the ion

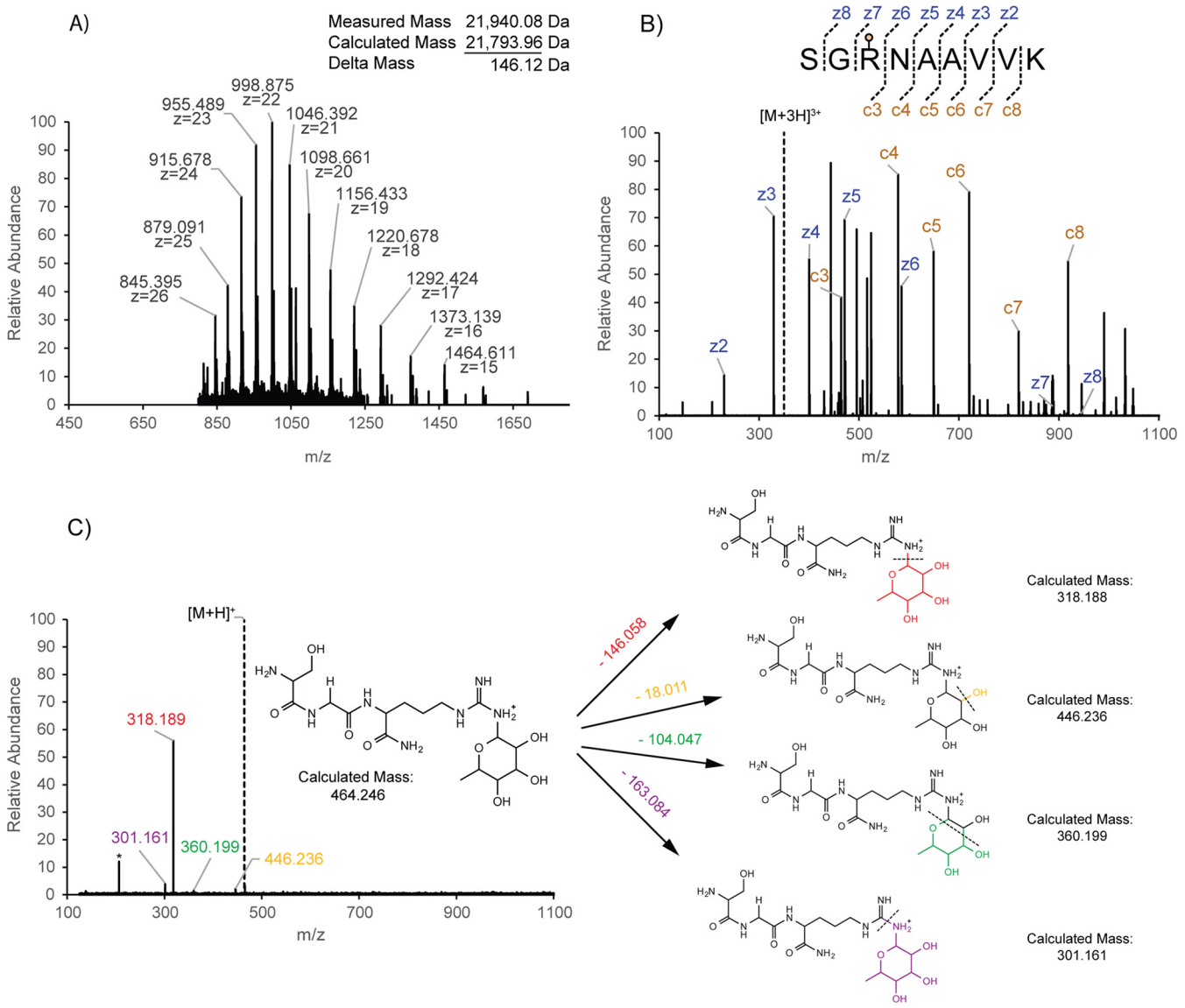

FIG 1 Mass spectrometry characterization of rhamnosylated EF-P. (A) A mass spectrum of His6–EF-P protein, recorded on a 7T FT-ICR instrument, from which protein molecular masses were calculated. (B) Lys-C-digested peptide fragmented by ETD maps the additional mass of 146.057 Da on Arg32. The precursor ion, *m/z* 349.865, is indicated by a dashed line. (C) A proposed fragmentation pattern based on ETD-HCD MS^3 data from the $c3^+$ ion. The neutral losses are colored uniquely to associate the fragment ion with the hypothetical structure. The asterisk indicates a background ion. The precursor ion, *m/z* 464.246, is indicated by a dashed line.

at *m/z* 104.047 matched the neutral loss of $C_4H_8O_3$ (see Table S2 and Fig. S3).

Mechanism of rhamnosylation of *P. aeruginosa* EF-P. Whereas, on the basis of mass concordance and fragmentation patterns, the mass spectrometry data strongly suggest that the modification represents a deoxyhexose, the possibility that the glycan is fucose rather than rhamnose cannot be excluded. Using the elemental composition as the input, the annotated genomes of *Pseudomonas* species in KEGG were searched for biosynthesis pathways of fucose and rhamnose (27, 28). Two sugar-nucleotide pathways were identified, each dedicated to the biosynthesis of a different rhamnose sugar-nucleotide isomer. The dTDP-L-rhamnose sugar nucleotide is formed through the conserved *rmlABCD*-encoded pathway, while the poorly conserved *rmd* oxidoreductase forms GDP-D-rhamnose (29). In addition, the genomic neighborhoods of *efp* in strains related to *P. aeruginosa* were searched, yielding a strongly conserved gene of unknown function, PA2852 (*earP*). The sequences of *rmlC*, *earP*, and *efp* coding the putatively modified arginine residue were used to search 2,723 bacterial genomes (see Fig. S4 in the supplemental material). Of the 252 species carrying *efp*, all contained *earP*, while 246 genomes carried *rmlC*. For the 6 species that do not carry *rmlC*, 2 are known to be obligate predators of *P. aeruginosa* and 4 obligate endosymbionts of trypanosomes (see Table S3).

Guided by the bioinformatics results, we generated *P. aeruginosa* strains with in-frame deletions of *earP* and *efp*, while a strain with a disrupted *rmlC* gene was obtained from a previous study (30). EF-P in *E. coli* has been reported to provide ribosomes with

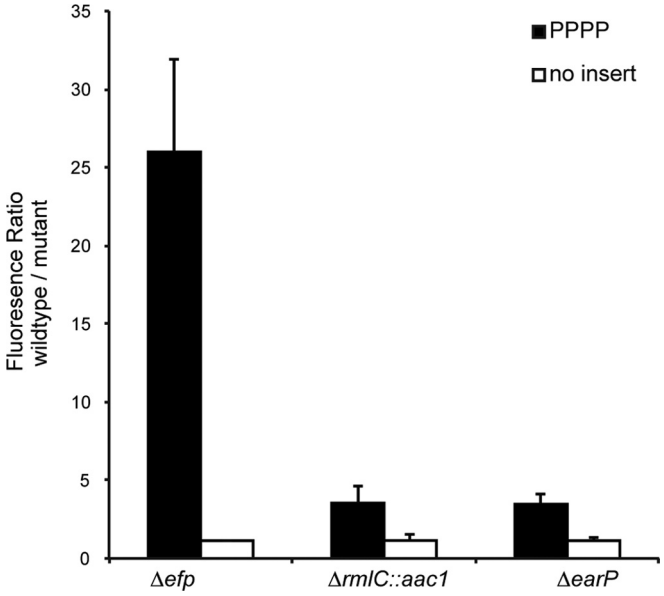

FIG 2 *P. aeruginosa* is dependent on EF-P to efficiently translate poly-proline motifs. *P. aeruginosa* strains deficient in EF-P activity were assessed using a Pro_4-GFP reporter (PPPP). Results represent cells grown in LB and collected at the mid-log phase and expressing the reporter. Error bars are the mean standard deviations of the results of three biological replicates.

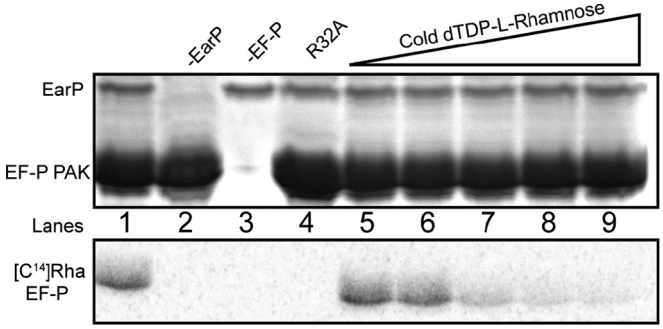

FIG 3 *In vitro* rhamnosylation of EF-P. Modification of recombinant EF-P was monitored over 30 min at 37°C with radioactive dTDP-L-[C^{14}]rhamnose (Rha) and resolved on an SDS-PAGE gel. The top image is of the Coomassie-stained SDS-PAGE gel, while the image below is the same gel dried and exposed on a phosphorimager after 24 h. A competition assay was performed with 10 μM to 1 mM cold dTDP-L-rhamnose.

assistance when translating consecutive proline codons. The translation efficiency of poly-prolines for each of the mutant strains was evaluated using a GFP-linked *in vivo* reporter system. On average, *rmlC*::*aac1*, Δ*earP*, and Δ*efp* showed 3.6-, 3.5-, and 25-fold decreases in GFP-Pro_4/mCherry levels compared to the wild type (WT), respectively (Fig. 2). Relative modification levels were directly assessed in each mutant strain by purifying His6–EF-P and subjecting the resulting proteins to mass spectrometric analyses. The majority (91%) of His6–EF-P was modified when it was purified from WT strains, while a complete absence of modification was observed for the *earP* mutant, and EF-P purified from *rmlC* strains yielded less than 5% modified protein (see Fig. S5 in the supplemental material).

The near-absence of modified EF-P from the *rmlC* mutant implicated dTDP-L-rhamnose as the substrate for rhamnose addition. Cell lysate-synthesized [^{14}C]dTDP-L-rhamnose was used in a reconstituted *in vitro* reaction with purified EarP and EF-P, and the rhamnosylation reaction, monitored over a period of 30 min, showed that EF-P was modified only when EarP, EF-P, and dTDP-L-rhamnose were all present (Fig. 3). In addition, R32A EF-P was not modified, confirming the site of the modification to be Arg32. The addition of unlabeled, commercially available dTDP-L-rhamnose outcompeted the radiolabeled modification reaction, confirming that [^{14}C]dTDP-L-rhamnose had been successfully prepared from crude lysate.

Physiological consequences of EF-P rhamnosylation. RmlC has been previously characterized as participating in the assembly of the core oligosaccharide, and deletion of the gene leads to altered lipopolysaccharide (LPS) and flagellum-mediated motility defects (31). In swimming motility assays, the *efp*, *earP*, and *rmlC* mutants all exhibited a significant 2-fold decrease in the zone traversed compared to the WT ($P < 0.0001$) (Fig. 4A). Vegetative growth defects were also similar for the mutants, with doubling times of about 100 min, while the WT strain and complemented Δ*efp* and Δ*rmlC* strains had doubling times of 45 and 50 min, respectively (Fig. 4C). The addition of either *efp*(*R32K*) or *efp*(*R32A*) in *trans* did not complement the growth phenotypes of the Δ*efp* strain but rather exacerbated them. Antibiotic susceptibility was determined by disc diffusion assays and revealed that antibiotics targeting cell wall synthesis exhibited significantly increased activity against the *efp*, *earP*, and *rmlC* mutants compared to that seen against the WT ($P < 0.005$), with ertapenem showing the most pronounced effects (Fig. 4B). Antibiotics targeting protein synthesis appeared to have no inhibitory effect on the mutants compared to the WT results.

DISCUSSION

Here we report a second example of EF-P rhamnosylation and further demonstrate that the rhamnose glycan exists in a cyclic confirmation, in contrast to the linear structures of β-Lys and hypusine (21). Even though an open-chain confirmation of rhamnose would allow a similar extent of protrusion into the peptidyl-transfer center, the stability of such a modification would be compromised, as Schiff bases are naturally unstable. Nevertheless, cyclic rhamnose is decorated with hydroxyl groups, which could provide additional hydrogen bonding with the P site tRNA and help restrict tRNA movement, while the β-Lys and hypusine modifications may directly interact with peptidyl-prolyl-tRNA to enhance the reactivity of the amino acceptor group.

Sugar modifications have rarely been studied with respect to translation factors, the only known example being monoglycosylation of EF1A by *Legionella pneumophila*, which suppresses global translation in the host organism (32). Our data show that the function of the rhamnose modification *in vivo* is to contribute to the efficiency of translating consecutive proline codons. We observed a range of intermediate effects on translation among the EF-P and modification mutants studied, suggesting that a compensatory mechanism exists when dTDP-L-rhamnose is not formed by *rmlC*. Additionally, a low but detectable level of modified EF-P was found in the Δ*rmlC*::*aac1* strain. One possible explanation is that GDP-D-rhamnose is utilized by EarP as a less efficient substrate, akin to α-lysine being used by PoxA in the absence of *yjeK*. Alternatively, RmlC could have retained low levels of activity after disruption with the gentamicin resistance gene cassette, allowing small quantities of EF-P to be modified.

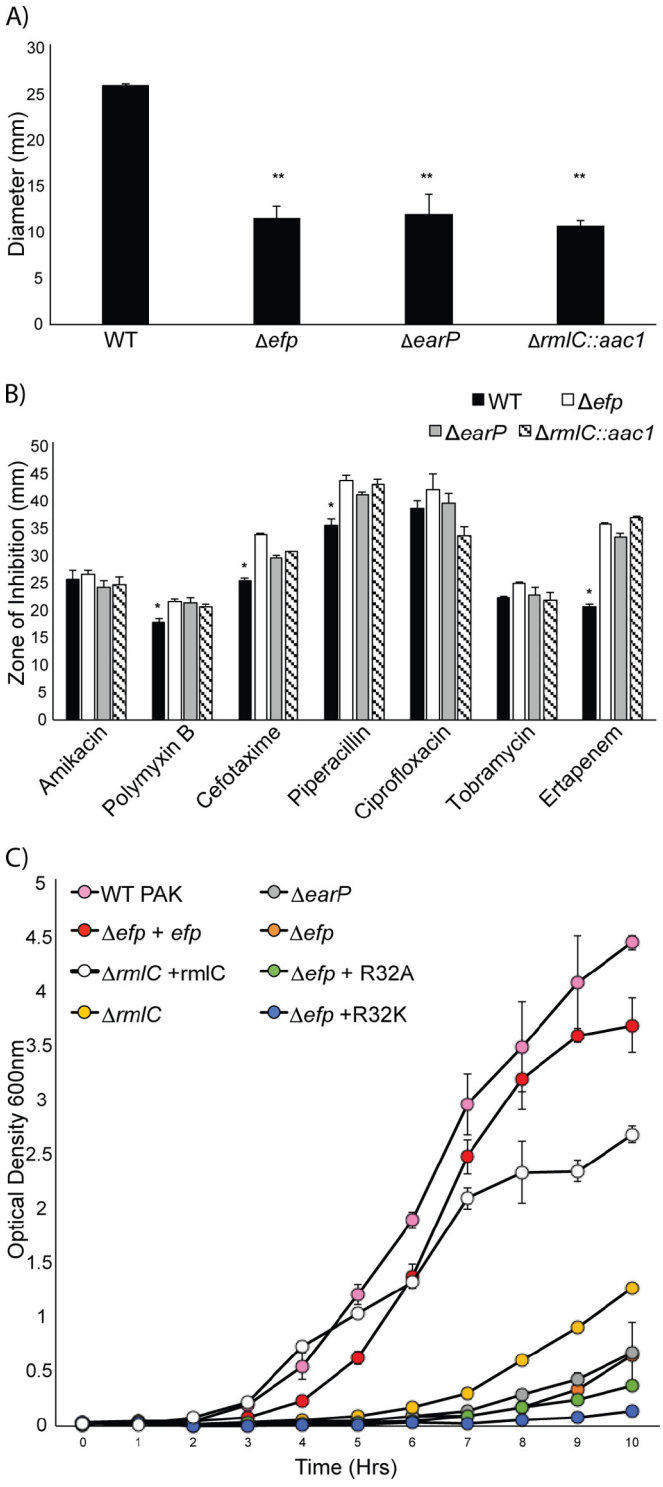

FIG 4 Defining the physiological role of the EF-P pathway in *P. aeruginosa*. (A) Swimming motility analyses were performed in triplicate, and data were determined by measuring the diameter of the colonies after a period of 24 h. ANOVA was used to determine statistical significance, which is represented by two adjacent asterisks. (B) Antibiotic susceptibility was tested by plating cultures of bacteria onto plates containing a variety of antibiotic discs targeting cellular membranes and protein synthesis. Antibiotic concentrations differed depending on the antibiotic, and analyses were conducted in three biological replicates. A single asterisk signifies that the results from all three mutant strains were found to be statistically significantly different from those from the

(Continued)

Our bioinformatics search (see Table S3 in the supplemental material) revealed that not all organisms harboring *efp* and *earP* genomically carry a complete *rmlABCD* operon. Notably, all organisms that lack a complete *rmlABCD* operon require a host for survival. For example, *Micavibrio aeruginosavorus* exists in two phases, an attack phase and an attachment phase, both of which have been transcriptionally characterized (33). Interestingly, *efp* and *earP* were transcriptionally silent during the attack phase, but during the attachment phase when *M. aeruginosavorus* interacted with *P. aeruginosa*, a burst of expression was observed for *efp* and *earP*. It is tempting to speculate that these obligate predators hijack the host's dTDP-L-rhamnose as a source to modify their own EF-P, which would define the host range for *M. aeruginosavorus*, if expression of poly-proline proteins is essential for predation.

Previous studies revealed swimming motility defects for *rmlC* mutants, but the impaired motility was attributed to the absence of rhamnosylated flagella and LPS (31). *P. aeruginosa* is rich in poly-proline sequences, having ~3-fold more poly-proline-containing proteins than *Salmonella* spp. (see Fig. S6 in the supplemental material). Putative EF-P targets (i.e., 3 or more consecutive Pro proteins) in *P. aeruginosa* include proteins involved with motility, protein synthesis, and DNA replication, making it reasonable to suggest that the swimming impairment observed in Δ*rmlC*::*aac1* strains could be partly due to diminished EF-P activity.

The fact that a variety of proteins depend on properly modified EF-P for efficient synthesis is consistent with the observation that *P. aeruginosa* strains mutated in *efp*, *earP*, and *rmlC* have prominent growth defects and increased sensitivity to antibiotics. The compounds with the largest effects against strains lacking EF-P or its modification were inhibitors of cell wall synthesis, while antibiotics targeting protein synthesis had the least effect. A possible explanation for the antibiotic susceptibility phenotype is that a necessary component for beta-lactam specificity, MexA, carries a triple-proline motif and may require EF-P for synthesis (34). Similar results were corroborated in a previous study; however, those experiments were conducted using Δ*efp*::*gent* PAO1 strains, which may explain the observed differences in antibiotic susceptibility (35).

The known EF-P glycosylation and lysylation pathways are identifiable in only about 30% of all bacterial genomes; the genomes of many of the bacteria apparently lacking such pathways, for instance, species of *Actinobacteria*, nevertheless encode a significantly higher number of poly-proline motifs than the majority of organisms in other bacterial phyla. This suggests that an even greater variety of EF-P posttranslational modification pathways may have evolved than have already been described. Further studies into the structurally diverse modifications of EF-P are now warranted to better understand the functional convergence of these different proteins in translational control.

MATERIALS AND METHODS

Bacterial strains and routine growth. Strains and plasmids are listed in Table S4 in the supplemental material. Bacteria were grown routinely in

Figure Legend Continued

WT strain according to an ANOVA. (C) Inocula of saturated overnight cultures were diluted 1,000-fold in LB, and growth curves were monitored over a period of 10 h, with measurements taken every hour. The graph represents averages of the results of three biological replicates, with errors bars representing the standard deviations of the means.

Luria-Bertani (LB) broth or on LB agar plates at 37°C. In some cases, *P. aeruginosa* was grown on Vogel Bonner minimal (VBM) base agar (Difco). All *P. aeruginosa* strains used were derived from strain PAK (36). *E. coli* K-12 strain SM10 was used for conjugation of plasmids into *P. aeruginosa* (37). The following concentrations of antibiotics were used: for ampicillin, 200 μg/ml for *E. coli*; for gentamicin, 15 μg/ml for *E. coli* and 75 μg/ml for *P. aeruginosa*; for carbenicillin, 150 μg/ml for *P. aeruginosa*; for spectinomycin, 50 μg/ml for *E. coli* and 500 μg/ml for *P. aeruginosa*; and for streptomycin, 50 μg/ml for *E. coli* and 250 μg/ml for *P. aeruginosa*.

Plasmid and strain constructions and mutagenesis. All PCR-generated plasmid insertion fragments were confirmed by DNA sequencing. *efp* and *earP* in-frame deletion mutants and a strain encoding His6–EF-P were constructed using the *sacB*$^+$ pEX18Ap suicide vector (38). For the in-frame deletion mutants, two ~500-bp fragments from the regions immediately upstream and downstream of the area to be deleted were amplified by PCR and cloned into the pEX18Ap vector. For the strain encoding His6-Efp, two ~500-bp fragments from the region immediately upstream and downstream of the second *efp* codon were amplified by PCR. The primers incorporated a region encoding His6 immediately downstream of the *efp* initiation codon and were joined by sewing overlap extension (SOE) PCR (39) and then cloned into pEX18Ap. The plasmids were integrated into the *P. aeruginosa* chromosome following conjugation from *E. coli*, and sucrose-resistant carbenicillin-sensitive segregants were isolated on agar containing 10% (wt/vol) sucrose. Deletions were verified by genomic PCR analysis using primers flanking the mutated region but outside the pEX18Ap clone insertion.

The pAJD2217 *araBp-His*$_6$*-efp* expression plasmid was constructed by amplifying *His*$_6$*-efp* from genomic DNA of strain AJDP739 and cloning it into plasmid pHERD20T. Mutagenesis of *His*$_6$*-efp* was performed using a QuikChange site-directed mutagenesis kit (Stratagene) to generate *efp*(R32A) and *efp*(R32K) in expression plasmids pAIR010 and pAIR015, respectively. T5*p-His*$_6$*-earP* expression plasmid pAJD2457 was constructed by amplifying *earP* lacking its initiation codon from the *P. aeruginosa* genome and cloning it into plasmid pQE30 as a BamHI-HindIII fragment. T7*p-rmlA* expression plasmid pAIR0017 was constructed by amplifying *rmlA* from *P. aeruginosa* genomic DNA and cloning it into a pET33b(+) plasmid as a EcoRI-NcoI fragment. *araBp-Pro*$_4$*-sfGFP-itagmCherry* and *araBp-sfGFP-itagmCherry* expression plasmids pAIR021 and pAIR023 were generated as a KpnI-EcoRI fragment and cloned into pHERD20T adapted from previously described templates (40, 41). *rmlC* was amplified from the PAK genome and cloned into pHERD20T to form the pAIR040 complementation plasmid.

Swimming motility assay. WT (PAK), Δ*efp*, Δ*rmlC*, and Δ*earP* *P. aeruginosa* strains were grown to saturation in Luria broth. Luria broth agar plates (0.3% agar) were poured on the day of use, with 28 ml media per plate. After plates had solidified for a minimum for 4 h, a toothpick dipped into the saturated culture penetrated halfway into the agar. Plates were incubated at 37°C for 24 h. After incubation, plates were imaged and the distance of migration was measured using VisionWorksLS acquisition and analysis software.

Antibiotic susceptibility assay. WT (PAK), Δ*efp*, Δ*rmlc*, and Δ*earP* *P. aeruginosa* strains were grown in Luria broth at 37°C with shaking to an optical density at 600 nm (OD_{600}) of 0.5. A sterile swab was dipped into the culture and streaked on a Luria broth agar plate in order to form a bacterial lawn. Oxoid antimicrobial susceptibility test discs were manually placed on the surface of the plate. Plates were incubated at 37°C for 24 h. After incubation, plates were imaged and the zone of inhibition was measured using VisionWorksLS acquisition and analysis software.

Bioinformatics and statistics. Genomic neighborhood clustering of *earP* was observed using SEEDViewer based on the protein sequence of *earP* from *Pseudomonas aeruginosa* PAO1 (42). BLAST searches of a database constructed from NCBI's 2,773 bacterial genomes (ftp://ftp.ncbi.nih.gov/genomes/Bacteria/) were performed for *earP*, *rmlC*, and *efp* (43). The presence of *rmlC*, *earP*, and *efp* was plotted across a taxonomic tree generated using ITOL (44). The statistical significance of the results of the motility and antibiotic assays was determined by performing an analysis of variance (ANOVA), and the resulting *P* values were corrected for multiple comparisons using a Dunnet test.

His-tagged purification of EarP and EF-P. XJB BL21(DE3) cells were used in all cases for recombinant protein expression. N-terminal His6–EF-P was expressed in LB supplemented with 0.2% arabinose and 150 μg/ml carbenicillin and grown for 16 h at 37°C. N-terminal His6-*earP* was expressed in LB by growing cells to the mid-log phase followed by induction with 1 mM IPTG (isopropyl-β-D-thiogalactopyranoside) and growth overnight at 20°C. Cells were pelleted at 7,500 × *g* for 10 min. Lysis of cell pellets and subsequent purification were carried out at 4°C with cells resuspended in lysis buffer (10 mM Tris-HCl [pH 7.4], 500 mM NaCl, 5 mM imidazole, and a single tablet of Roche Complete protease inhibitor) and lysed by sonication. Lysate was clarified at 75,600 × *g* and loaded onto a gravity column with Talon resin. The column was washed with 50 column volumes of wash buffer (10 mM Tris-HCl [pH 7.4], 500 mM NaCl, 5 mM imidazole) and eluted with wash buffer supplemented with 200 mM imidazole. Elutent fractions were pooled, concentrated, and dialyzed against 10 mM Tris (pH 7.4)–100 mM NaCl–2 mM BME (β-mercaptoethanol)–10% glycerol.

Modification characterization by high-resolution mass spectrometry. His6–EF-P was purified from strains lacking *efp* or *earP* in an individual manner and subjected to liquid chromatography-tandem mass spectrometry (LC-MS$^+$) using a triple-quadrupole mass spectrometer (API III+; Applied Biosystems) connected to an in-line fraction collection device using a method adapted from previous reports (45, 46). Samples were injected onto a polymeric reversed-phase column (Polymer Labs) (PLRP/S; 5 μm pore size, 300 Å, 2 by 150 mm, 40°C) previously equilibrated in 95% buffer A and 5% buffer B (buffer A, 0.1% formic acid–water; buffer B, 0.1% formic acid–50% acetonitrile–50% isopropanol) and eluted (100 μl/min) with increasing percentages of buffer B (0 min/5% buffer B, 5 min/5% buffer B, 45 min/90% buffer B). Fractions were collected into microcentrifuge tubes and stored at −20°C for further analysis. Data were processed using MacSpec 3.3, Hypermass, and BioMultiview 1.3.1 software to determine which fractions contained EF-P (Applied Biosystems).

Selected high-performance LC (HPLC) fractions collected during LC-MS$^+$ were introduced into the FT-ICR instrument by a direct infusion nanospray method, as performed before (45). All samples were analyzed using a hybrid linear ion-trap/FT-ICR mass spectrometer (7T, LTQ FT Ultra; Thermo Scientific) operated with a standard (up to *m*/*z* 2,000) or extended (up to *m*/*z* 4,000) mass range. Spectra were derived from an average of between 100 and 400 transient signals. Data were analyzed using ProSight PC software (Thermo Fisher).

Samples were proteolytically digested with Lys-C (Promega) and diluted (1/10) into a 30% acetonitrile–1% acetic acid solution, and 5 μl to 10 μl of the dilution was loaded into a Picotip (New Objective) metal-coated static nanospray tip (2 μm tip inner diameter [ID]). The nanospray tip was placed in a FlexSpray stage (Thermo Scientific) that was attached to an Orbitrap Elite mass spectrometer with ETD (electron transfer dissociation) (Thermo Scientific), and a 1.5-kV spray voltage was applied to generate the electrospray. Data were manually collected using Orbitrap Tune Plus software, and the capillary temperature was set to 300°C. MS1 data were collected in the Orbitrap with a resolution value of 240,000, an automatic gain control (AGC) target of 1E6 ions, and an injection time of 250 ms. MS^2 data were generated by ETD with a 100-ms activation time, and data were collected in the Orbitrap with a resolution value of 240,000, an AGC target value of 5E4 ions, and an injection time of 250 ms. MS^3 data were collected by selecting an ion of interest from the MS^2 data and further fragmenting it by higher-energy collision-induced dissociation (HCD) and collecting the data in the Orbitrap mass analyzer (under conditions identical to the MS^2 conditions). All data acquisition was performed for 1-min intervals.

Estimation of rhamnosylated EF-P levels. Three hundred nanograms of peptides was separated by reverse-phase HPLC (Dionex) on a C_{18AQ} column (Michrom Bioresources Inc.) (0.2 mm by 150 mm, 3 μm pore size, 200 Å) coupled to an LTQ Orbitrap XL instrument (Thermo Fisher Scientific). In all cases, peptide separation was accomplished with water (buffer A) and acetonitrile (buffer B) with the addition of 0.1% formic acid as an ion-pairing agent. Peptides were loaded onto an Acclaim PepMap100 C_{18} trap cartridge (Dionex) (0.3 mm by 5 mm, 5 μm pore size, 100 Å) and washed with 5% buffer B for 3 min. Peptides were eluted at a flow rate of 2 μl/min with an increasing linear gradient of 5% to 30% buffer B over 47 min. The column was subsequently washed with 90% buffer B for 5 min, and the system was equilibrated for 10 min prior to performing an independent system wash to ascertain sample carryover.

An LTQ Orbitrap XL instrument was used to identify and estimate levels of both modified and unmodified forms of *P. aeruginosa* EF-P. Peptides were ionized using a captive spray ionization source (Michrom Bioresources Inc.) with an ionization voltage and a capillary temperature of 2.0 kV and 175°C, respectively. Positive-ion data acquisition was performed in a data-dependent fashion with dynamic exclusion and preview modes enabled. The top 5 precursor ions were selected for fragmentation with dynamic exclusion settings as follows: repeat count, 2; repeat duration, 20 s; exclusion list size, 100 entries; exclusion duration, 60 s; exclusion mass width, ±1.50 *m/z*. Precursor ions underwent collision-induced dissociation fragmentation in the LTQ linear ion trap with a normalized collision energy (NCE) level of 35%. RAW data were converted to mzXML files using MSConvert (47, 48) and searched with MassMatrix (49, 50) against a UniProt *P. aeruginosa* PAO1 proteome concatenated with modified forms of the EF-P sequence. To differentiate between rhamnosylated and nonrhamnosylated EF-P, extracted-ion chromatograms (XIC) were produced from the 3+ charged species containing unique transitions. The yield of rhamnosylated EF-P was estimated by quantifying the corresponding XIC peaks. Quantification was performed using Thermo Xcalibur version 2.0 with Genesis algorithm peak detection and a smoothing value of 5.

***In vivo* reporter.** Overnight LB cultures of strains harboring the reporter construct were inoculated into fresh LB media containing 0.2% arabinose for induction or into LB media without arabinose (to serve as a control for background fluorescence). Once the log phase was reached, 1 ml of cells was collected and washed 3 times with 1× phosphate-buffered saline solution to remove excess LB, which has a strong emission signal at the same wavelength as GFP (51). Fluorescence readings for GFP and mCherry were measured using a Fluorolog-3 instrument as described previously (41, 52).

Enzymatic synthesis of dTDP-[^{14}C]rhamnose. dTDP-[^{14}C]Rha was prepared from [U^{14}C]sucrose (PerkinElmer) as described previously (53), with minor alterations. The reaction was carried out with 50 μCi (442/mCi/mmol, 113 nmol) of vacuum-dried [U-^{14}C]sucrose, 40 mM KH_2PO_4 (pH 7.0), 0.5 U of sucrose phosphorylase (Sigma), 1 mM TTP, 2 U of inorganic pyrophosphatase (Roche), 0.5 mg of lysate from XJB BL21(DE3) cells expressing *rmlA*, 875 μM NADPH, 50 mM HEPES buffer at pH 7.0, and 10 mM $MgCl_2$. After 1 h of incubation at 37°C, the reaction mixture was supplemented with 200 μl of crude *E. coli* XJB BL21(DE3) lysate grown to the mid-log phase and an additional 35 μl of 10 mM NADPH was reacted at 37°C for another 30 min. The reaction mixture was then filtered using an Amicon Ultra-0.5 3-kDa centrifugal filter device and vacuum dried to a final volume of 250 μl.

***In vitro* rhamnosylation of EF-P.** The *in vitro* reaction mixture was composed of purified His6-EarP and His6–EF-P, dTDP[^{14}C]rhamnose, 1 mM $MgCl_2$, 10 mM Tris-HCl (pH 7.5), and 100 mM NaCl, unless otherwise stated. Competition assays were performed in the presence of cold dTDP-L-rhamnose (Carbosynth) at concentrations ranging from 100 μM to 1 mM. All reactions were carried out at 37°C for 30 min, and all reaction mixtures were quenched in 5× sodium dodecyl sulfate-polyacrylamide gel electrophoresis loading buffer. Reactions were then run on a 14% SDS-PAGE gel, and radioactivity was detected by phosphorimaging.

SUPPLEMENTAL MATERIAL

Supplemental material for this article may be found at http://mbio.asm.org/lookup/suppl/doi:10.1128/mBio.00823-15/-/DCSupplemental.

Figure S1, PDF file, 0.1 MB.
Figure S2, PDF file, 0.2 MB.
Figure S3, PDF file, 0.1 MB.
Figure S4, PDF file, 0.2 MB.
Figure S5, PDF file, 0.3 MB.
Figure S6, PDF file, 0.1 MB.
Table S1, PDF file, 0.2 MB.
Table S2, PDF file, 0.1 MB.
Table S3, PDF file, 0.3 MB.
Table S4, PDF file, 0.5 MB.

ACKNOWLEDGMENTS

We thank Joseph Lam for his kind contribution of the Δ*rmlC*::*acc1* strain and Lisa Jones for assistance with Orbitrap Elite data collection.

This work was supported by a grant from the National Institutes of Health to M.I. (GM065183), and W.N. received support from the Natural Sciences and Engineering Research Council of Canada (NSERC) (RGPIN-2015-05292). A.J.D. holds an Investigators in Pathogenesis of Infectious Disease award from the Burroughs Wellcome Fund. The FHCRC Proteomics Facility is partially funded by Cancer Center Support grant P30 CA015704 from the National Institutes of Health. J.P.W. acknowledges support from the UCSD/UCLA NIDDK Diabetes Research Center (P30 DK063491).

REFERENCES

1. **Starosta AL, Lassak J, Jung K, Wilson DN**. 2014. The bacterial translation stress response. FEMS Microbiol Rev **38:**1172–1201. http://dx.doi.org/10.1111/1574-6976.12083.
2. **Boël G, Smith PC, Ning W, Englander MT, Chen B, Hashem Y, Testa AJ, Fischer JJ, Wieden H-J, Frank J, Gonzalez RL, Hunt JF**. 2014. The ABC-F protein EttA gates ribosome entry into the translation elongation cycle. Nat Struct Mol Biol **21:**143–151. http://dx.doi.org/10.1038/nsmb.2740.
3. **Chen B, Boël G, Hashem Y, Ning W, Fei J, Wang C, Gonzalez RL, Jr, Hunt JF, Frank J**. 2014. EttA regulates translation by binding the ribosomal E site and restricting ribosome-tRNA dynamics. Nat Struct Mol Biol **21:**152–159. http://dx.doi.org/10.1038/nsmb.2741.
4. **Traxler MF, Summers SM, Nguyen HT, Zacharia VM, Hightower GA, Smith JT, Conway T**. 2008. The global, ppGpp-mediated stringent response to amino acid starvation in *Escherichia coli*. Mol Microbiol **68:**1128–1148. http://dx.doi.org/10.1111/j.1365-2958.2008.06229.x.
5. **Wendrich TM, Blaha G, Wilson DN, Marahiel MA, Nierhaus KH**. 2002. Dissection of the mechanism for the stringent factor RelA. Mol Cell **10:**779–788. http://dx.doi.org/10.1016/S1097-2765(02)00656-1.
6. **Sørensen MA**. 2001. Charging levels of four tRNA species in *Escherichia coli* Rel(+) and Rel(−) strains during amino acid starvation: a simple model for the effect of ppGpp on translational accuracy. J Mol Biol **307:**785–798. http://dx.doi.org/10.1006/jmbi.2001.4525.
7. **Navarre WW, Zou SB, Roy H, Xie JL, Savchenko A, Singer A, Edvokimova E, Prost LR, Kumar R, Ibba M, Fang FC**. 2010. PoxA, yjeK, and elongation factor P coordinately modulate virulence and drug resistance in *Salmonella enterica*. Mol Cell **39:**209–221. http://dx.doi.org/10.1016/j.molcel.2010.06.021.
8. **Balakrishnan R, Oman K, Shoji S, Bundschuh R, Fredrick K**. 2014. The conserved GTPase LepA contributes mainly to translation initiation in *Escherichia coli*. Nucleic Acids Res **42:**13370–13383. http://dx.doi.org/10.1093/nar/gku1098.
9. **Bullwinkle TJ, Zou SB, Rajkovic A, Hersch SJ, Elgamal S, Robinson N, Smil D, Bolshan Y, Navarre WW, Ibba M**. 2013. (R)-beta-lysine-modified elongation factor P functions in translation elongation. J Biol Chem **288:**4416–4423. http://dx.doi.org/10.1074/jbc.M112.438879.
10. **Zou SB, Roy H, Ibba M, Navarre WW**. 2011. Elongation factor P mediates a novel post-transcriptional regulatory pathway critical for bacterial virulence. Virulence **2:**147–151. http://dx.doi.org/10.4161/viru.2.2.15039.
11. **Sajid A, Arora G, Gupta M, Singhal A, Chakraborty K, Nandicoori VK, Singh Y**. 2011. Interaction of *Mycobacterium tuberculosis* elongation factor

Tu with GTP is regulated by phosphorylation. J Bacteriol **193:**5347–5358. http://dx.doi.org/10.1128/JB.05469-11.
12. **Dworkin J.** 2015. Ser/Thr phosphorylation as a regulatory mechanism in bacteria. Curr Opin Microbiol **24:**47–52. http://dx.doi.org/10.1016/j.mib.2015.01.005.
13. **Germain E, Castro-Roa D, Zenkin N, Gerdes K.** 2013. Molecular mechanism of bacterial persistence by HipA. Mol Cell **52:**248–254. http://dx.doi.org/10.1016/j.molcel.2013.08.045.
14. **Kaspy I, Rotem E, Weiss N, Ronin I, Balaban NQ, Glaser G.** 2013. HipA-mediated antibiotic persistence via phosphorylation of the glutamyl-tRNA-synthetase. Nat Commun **4:**3001. http://dx.doi.org/10.1038/ncomms4001.
15. **Bearson SM, Bearson BL, Brunelle BW, Sharma VK, Lee IS.** 2011. A mutation in the poxA gene of *Salmonella enterica* serovar Typhimurium alters protein production, elevates susceptibility to environmental challenges, and decreases swine colonization. Foodborne Pathog Dis **8:**725–732. http://dx.doi.org/10.1089/fpd.2010.0796.
16. **Roy H, Zou SB, Bullwinkle TJ, Wolfe BS, Gilreath MS, Forsyth CJ, Navarre WW, Ibba M.** 2011. The tRNA synthetase paralog PoxA modifies elongation factor-P with (R)-beta-lysine. Nat Chem Biol **7:**667–669. http://dx.doi.org/10.1038/nchembio.632.
17. **Peil L, Starosta AL, Lassak J, Atkinson GC, Virumäe K, Spitzer M, Tenson T, Jung K, Remme J, Wilson DN.** 2013. Distinct XPPX sequence motifs induce ribosome stalling, which is rescued by the translation elongation factor EF-P. Proc Natl Acad Sci U S A **110:**15265–15270. http://dx.doi.org/10.1073/pnas.1310642110.
18. **Doerfel LK, Wohlgemuth I, Kothe C, Peske F, Urlaub H, Rodnina MV.** 2013. EF-P is essential for rapid synthesis of proteins containing consecutive proline residues. Science **339:**85–88. http://dx.doi.org/10.1126/science.1229017.
19. **Gutierrez E, Shin BS, Woolstenhulme CJ, Kim JR, Saini P, Buskirk AR, Dever TE.** 2013. eIF5A promotes translation of polyproline motifs. Mol Cell **51:**35–45. http://dx.doi.org/10.1016/j.molcel.2013.04.021.
20. **Cooper HL, Park MH, Folk JE, Safer B, Braverman R.** 1983. Identification of the hypusine-containing protein hy+ as translation initiation factor eIF-4D. Proc Natl Acad Sci U S A **80:**1854–1857. http://dx.doi.org/10.1073/pnas.80.7.1854.
21. **Lassak J, Keilhauer EC, Fürst M, Wuichet K, Gödeke J, Starosta AL, Chen JM, Søgaard-Andersen L, Rohr J, Wilson DN, Häussler S, Mann M, Jung K.** 2015. Arginine-rhamnosylation as new strategy to activate translation elongation factor P. Nat Chem Biol **11:**266–270. http://dx.doi.org/10.1038/nchembio.1751.
22. **Haltiwanger RS, Lowe JB.** 2004. Role of glycosylation in development. Annu Rev Biochem **73:**491–537. http://dx.doi.org/10.1146/annurev.biochem.73.011303.074043.
23. **Tytgat HL, Lebeer S.** 2014. The sweet tooth of bacteria: common themes in bacterial glycoconjugates. Microbiol Mol Biol Rev **78:**372–417. http://dx.doi.org/10.1128/MMBR.00007-14.
24. **Creasy DM, Cottrell JS.** 2004. Unimod: protein modifications for mass spectrometry. Proteomics **4:**1534–1536. http://dx.doi.org/10.1002/pmic.200300744.
25. **Fedorova M, Frolov A, Hoffmann R.** 2010. Fragmentation behavior of Amadori-peptides obtained by non-enzymatic glycosylation of lysine residues with ADP-ribose in tandem mass spectrometry. J Mass Spectrom JMS **45:**664–669. http://dx.doi.org/10.1002/jms.1758.
26. **Horai H, Arita M, Kanaya S, Nihei Y, Ikeda T, Suwa K, Ojima Y, Tanaka K, Tanaka S, Aoshima K, Oda Y, Kakazu Y, Kusano M, Tohge T, Matsuda F, Sawada Y, Hirai MY, Nakanishi H, Ikeda K, Akimoto N, Maoka T, Takahashi H, Ara T, Sakurai N, Suzuki H, Shibata D, Neumann S, Iida T, Tanaka K, Funatsu K, Matsuura F, Soga T, Taguchi R, Saito K, Nishioka T.** 2010. MassBank: a public repository for sharing mass spectral data for life sciences. J Mass Spectrom **45:**703–714. http://dx.doi.org/10.1002/jms.1777.
27. **Kanehisa M, Goto S.** 2000. KEGG: Kyoto encyclopedia of genes and genomes. Nucleic Acids Res **28:**27–30. http://dx.doi.org/10.1093/nar/28.1.27.
28. **Kanehisa M, Goto S, Sato Y, Kawashima M, Furumichi M, Tanabe M.** 2014. Data, information, knowledge and principle: back to metabolism in KEGG. Nucleic Acids Res **42:**D199–D205. http://dx.doi.org/10.1093/nar/gkt1076.
29. **Lam JS, Taylor VL, Islam ST, Hao Y, Kocíncová D.** 2011. Genetic and functional diversity of *Pseudomonas aeruginosa* lipopolysaccharide. Front Microbiol **2:**118. http://dx.doi.org/10.3389/fmicb.2011.00118.
30. **Rahim R, Burrows LL, Monteiro MA, Perry MB, Lam JS.** 2000. Involvement of the rml locus in core oligosaccharide and O polysaccharide assembly in *Pseudomonas aeruginosa*. Microbiology **146:**2803–2814.
31. **Lindhout T, Lau PC, Brewer D, Lam JS.** 2009. Truncation in the core oligosaccharide of lipopolysaccharide affects flagella-mediated motility in *Pseudomonas aeruginosa* PAO1 via modulation of cell surface attachment. Microbiology **155:**3449–3460. http://dx.doi.org/10.1099/mic.0.030510-0.
32. **Belyi Y, Niggeweg R, Opitz B, Vogelsgesang M, Hippenstiel S, Wilm M, Aktories K.** 2006. *Legionella pneumophila* glucosyltransferase inhibits host elongation factor 1A. Proc Natl Acad Sci U S A **103:**16953–16958. http://dx.doi.org/10.1073/pnas.0601562103.
33. **Wang Z, Kadouri DE, Wu M.** 2011. Genomic insights into an obligate epibiotic bacterial predator: *Micavibrio aeruginosavorus* ARL-13. BMC Genomics **12:**453. http://dx.doi.org/10.1186/1471-2164-12-453.
34. **Li XZ, Nikaido H, Poole K.** 1995. Role of mexA-mexB-oprM in antibiotic efflux in *Pseudomonas aeruginosa*. Antimicrob Agents Chemother **39:**1948–1953. http://dx.doi.org/10.1128/AAC.39.9.1948.
35. **Balibar CJ, Iwanowicz D, Dean CR.** 2013. Elongation factor P is dispensable in *Escherichia coli* and *Pseudomonas aeruginosa*. Curr Microbiol **67:**293–299. http://dx.doi.org/10.1007/s00284-013-0363-0.
36. **Strom MS, Lory S.** 1986. Cloning and expression of the pilin gene of *Pseudomonas aeruginosa* PAK in *Escherichia coli*. J Bacteriol **165:**367–372.
37. **Miller VL, Mekalanos JJ.** 1988. A novel suicide vector and its use in construction of insertion mutations: osmoregulation of outer membrane proteins and virulence determinants in *Vibrio cholerae* requires toxR. J Bacteriol **170:**2575–2583.
38. **Choi KH, Schweizer HP.** 2005. An improved method for rapid generation of unmarked *Pseudomonas aeruginosa* deletion mutants. BMC Microbiol **5:**30. http://dx.doi.org/10.1186/1471-2180-5-30.
39. **Alm RA, Mattick JS.** 1995. Identification of a gene, pilV, required for type 4 fimbrial biogenesis in *Pseudomonas aeruginosa*, whose product possesses a pre-pilin-like leader sequence. Mol Microbiol **16:**485–496. http://dx.doi.org/10.1111/j.1365-2958.1995.tb02413.x.
40. **Henriques MX, Catalão MJ, Figueiredo J, Gomes JP, Filipe SR.** 2013. Construction of improved tools for protein localization studies in *Streptococcus pneumoniae*. PLoS One **8:**e55049. http://dx.doi.org/10.1371/journal.pone.0055049.
41. **Elgamal S, Katz A, Hersch SJ, Newsom D, White P, Navarre WW, Ibba M.** 2014. EF-P dependent pauses integrate proximal and distal signals during translation. PLoS Genet **10:**e1004553. http://dx.doi.org/10.1371/journal.pgen.1004553.
42. **Overbeek R, Olson R, Pusch GD, Olsen GJ, Davis JJ, Disz T, Edwards RA, Gerdes S, Parrello B, Shukla M, Vonstein V, Wattam AR, Xia F, Stevens R.** 2014. The SEED and the rapid annotation of microbial genomes using subsystems technology (RAST). Nucleic Acids Res **42:**D206–D214. http://dx.doi.org/10.1093/nar/gkt1226.
43. **Boratyn GM, Camacho C, Cooper PS, Coulouris G, Fong A, Ma N, Madden TL, Matten WT, McGinnis SD, Merezhuk Y, Raytselis Y, Sayers EW, Tao T, Ye J, Zaretskaya I.** 2013. BLAST: a more efficient report with usability improvements. Nucleic Acids Res **41:**W29–W33. http://dx.doi.org/10.1093/nar/gkt282.
44. **Letunic I, Bork P.** 2011. Interactive tree of life v2: online annotation and display of phylogenetic trees made easy. Nucleic Acids Res **39:**W475–W478. http://dx.doi.org/10.1093/nar/gkr201.
45. **Whitelegge JP, Zabrouskov V, Halgand F, Souda P, Bassilian S, Yan W, Wolinsky L, Loo JA, Wong DT, Faull KF.** 2007. Protein-sequence polymorphisms and post-translational modifications in proteins from human saliva using top-down Fourier-transform ion cyclotron resonance mass spectrometry. Int J Mass Spectrom **268:**190–197. http://dx.doi.org/10.1016/j.ijms.2007.08.008.
46. **Gómez SM, Nishio JN, Faull KF, Whitelegge JP.** 2002. The chloroplast grana proteome defined by intact mass measurements from liquid chromatography mass spectrometry. Mol Cell Proteomics **1:**46–59. http://dx.doi.org/10.1074/mcp.M100007-MCP200.
47. **Chambers MC, Maclean B, Burke R, Amodei D, Ruderman DL, Neumann S, Gatto L, Fischer B, Pratt B, Egertson J, Hoff K, Kessner D, Tasman N, Shulman N, Frewen B, Baker TA, Brusniak MY, Paulse C, Creasy D, Flashner L, Kani K, Moulding C, Seymour SL, Nuwaysir LM, Lefebvre B, Kuhlmann F, Roark J, Rainer P, Detlev S, Hemenway T, Huhmer A, Langridge J, Connolly B, Chadick T, Holly K, Eckels J, Deutsch EW, Moritz RL, Katz JE, Agus DB, MacCoss M, Tabb DL, Mallick P.** 2012. A cross-platform toolkit for mass spectrometry and proteomics. Nat Biotechnol **30:**918–920. http://dx.doi.org/10.1038/nbt.2377.

48. **Kessner D, Chambers M, Burke R, Agus D, Mallick P**. 2008. ProteoWizard: open source software for rapid proteomics tools development. BioInformatics **24:**2534–2536. http://dx.doi.org/10.1093/bioinformatics/btn323.
49. **Xu H, Freitas MA**. 2009. Automated diagnosis of LC-MS/MS performance. BioInformatics **25:**1341–1343. http://dx.doi.org/10.1093/bioinformatics/btp155.
50. **Xu H, Freitas MA**. 2009. MassMatrix: a database search program for rapid characterization of proteins and peptides from tandem mass spectrometry data. Proteomics **9:**1548–1555. http://dx.doi.org/10.1002/pmic.200700322.
51. **Doherty GP, Bailey K, Lewis PJ**. 2010. Stage-specific fluorescence intensity of GFP and mCherry during sporulation in *Bacillus subtilis*. BMC Res Notes **3:**303. http://dx.doi.org/10.1186/1756-0500-3-303.
52. **Hersch SJ, Wang M, Zou SB, Moon KM, Foster LJ, Ibba M, Navarre WW**. 2013. Divergent protein motifs direct elongation factor P-mediated translational regulation in *Salmonella enterica* and *Escherichia coli*. mBio **4:**e00180-13. http://dx.doi.org/10.1128/mBio.00180-13.
53. **Kang YB, Yang YH, Lee KW, Lee SG, Sohng JK, Lee HC, Liou K, Kim BG**. 2006. Preparative synthesis of dTDP-L-rhamnose through combined enzymatic pathways. Biotechnol Bioeng **93:**21–27. http://dx.doi.org/10.1002/bit.20648.